Inorganic Chemistry

Article

pubs.acs.org/IC

Expanded Porous Metal–Organic Frameworks by SCSC: Organic Building Units Modifying and Enhanced Gas-Adsorption Properties

Weidong Fan, Huan Lin, Xue Yuan, Fangna Dai,* Zhenyu Xiao, Liangliang Zhang,* Liwen Luo,* and Rongming Wang

State Key Laboratory of Heavy Oil Processing, College of Science, China University of Petroleum (East China), Qingdao, Shandong 266580, People's Republic of China

Supporting Information

ABSTRACT: Two amino-functional copper metal–organic frameworks of formula $[Cu_3(ATTCA)_2(H_2O)_3]\cdot 2DMF\cdot 11H_2O\cdot 12EtOH$ (**1**) (H_3ATTCA = 2-amino-[1,1:3,1-terphenyl]-4,4,5-tricarboxylic acid, pyz = pyrazine, DMF = dimethylformamide) and $[Cu_3(ATTCA)_2(pyz)(H_2O)]\cdot 2DMF\cdot 12H_2O\cdot 8EtOH$ (**2**) were synthesized under solvothermal conditions and characterized by single-crystal X-ray diffraction, infrared spectroscopy, elemental analyses, thermogravimetric analyses, and powder X-ray diffraction. Single-crystal X-ray diffraction analysis revealed that both complexes **1** and **2** are built of the $Cu_2(COO)_4$ paddlewheel secondary building units with an ***fmj*** topology. Importantly, complex **1** can be transformed into complex **2** by the single-crystal to single-crystal transformation of which the coordinated water molecules are replaced with pyz molecules. However, the adsorption abilities of **2** are obviously lower than those of **1**, as its pores are partially blocked by pyz molecules. Moreover, gas-adsorption analysis showed that the amino-functional **1** possesses higher gas-adsorption capacity than UMCM-151 for N_2, H_2, CH_4, and C_2H_2, especially for CO_2.

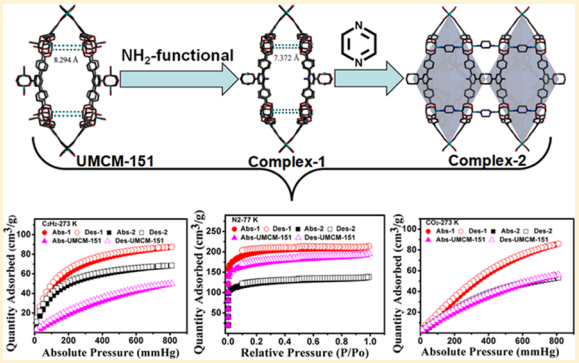

INTRODUCTION

As an emerging class of porous crystalline materials, metal–organic frameworks (MOFs) have attracted broad interests due to their various architectures,[1,2] high porosity,[3,4] and potential utilization in gas adsorption/separation,[5] catalysis,[6,7] luminescence,[8,9] magnetism,[10−13] and so on.[14,15] For most of the reported studies, gas adsorption/separation played an important role in MOF areas. Over the past decades, the frameworks with various pore size, shape, and chemical functionality have been developed by the extension or decoration of larger bridging ligands,[16−18] the utilization of highly connected secondary building units (SBUs),[19,20] and the modification of the complexes, such as postsynthetic methods and single-crystal to single-crystal (SCSC) transformation.[21−23]

The rational design or construction of functionalized MOFs can be conducted through the introduction of functional groups.[24] Chemists have realized that the amino-functional frameworks have better gas-adsorption abilities, especially for CO_2.[25] For example, Bai and Zaworotko groups demonstrated that the decorated MOFs with polar acylamide groups can significantly enhance the CO_2 binding ability and gas-adsorption selectivity;[26] Long and co-workers reported an amino-functional MOF with an exceptionally high adsorption capacity for CO_2 at low pressures.[27] Meanwhile, theoretical calculations also confirmed this concept.[28,29]

The paddlewheel cluster $[M_2(COO)_4]$ (M = Cu^{2+}, Zn^{2+}, Ni^{2+}) is the most well-known SBU among the reported metal-carboxylate MOFs,[30−33] where the axial locations are dominated by organic ligands or solvent molecules. On the basis of paddlewheel SBUs, the frameworks can be further expanded into complicated complexes by SCSC or adding the organic bridging ligands.[34,35] For example, the paddlewheel SBUs were connected through 1,4-diazabicyclo[2.2.2]octane (DABCO) or 4,4′-bipyridine (BPY) in the reported works, as the coordination ability of tertiary amine and pyridine are stronger than the coordinated solvent molecules.[36−39] However, the breaking/forming of coordination bonds is still a challenge for those transformations.[40] Susumu Kitagawa's group has made great contributions in this aspect, but some of their reports are based on removing the coordinated solvent molecules to form the vacant coordination sites.[41]

We are interested in the construction of new porous frameworks with multifunctional groups that possess better gas-adsorption properties.[42−44] Hence, the amino-functional ligand is designed, and the relevant complexes $[Cu_3(ATTCA)_2(H_2O)_3]\cdot 2DMF\cdot 11H_2O\cdot 12EtOH$ (**1**) and $[Cu_3(ATTCA)_2(pyz)(H_2O)]\cdot 2DMF\cdot 12H_2O\cdot 8EtOH$ (**2**) are synthesized (H_3ATTCA = 2-amino-[1,1:3,1-terphenyl]-4,4,5-tricarboxylic acid, pyz = pyrazine, DMF = dimethylformamide). It is interesting that complex **1** can be turned into **2** by the SCSC transformation of replacing the coordinated water molecules

Received: February 9, 2016
Published: June 17, 2016

DOI: 10.1021/acs.inorgchem.6b00278
Inorg. Chem. 2016, 55, 6420−6425

with pyz molecules. Since the amino-functional ligand of H_3ATTCA is used, **1** shows better gas-adsorption abilities for N_2, H_2, CO_2, C_2H_2, and CH_4 than the reported **UMCM-151**, which is assembled by the nonamino-functional ligand of [1,1:3,1-terphenyl]-4,4,5-tricarboxylic acid (H_3TTCA).[45] However, the gas-adsorption ability of **2** is lower than that of **UMCM-151**, as its pores are partially blocked by pyz molecules.

EXPERIMENTAL SECTION

Materials and General Methods. H_3ATTCA ligand was synthesized according to the route shown in Scheme 1, while Scheme 2 showed the synthetic procedures of the complexes **1**, **2**, and **UMCM-151**. The detailed procedures for synthesis of the ligand and complexes are listed in Supporting Information.[46] All the solvents and materials were purchased from chemical vendors and without further depuration before used. The powder X-ray diffraction (XRD) diffractograms were obtained on a Panalytical X-Pert pro diffractometer with Cu Kα radiation. Elemental analyses (C, H, N) were performed using a CE instruments EA 1110 elemental analyzer. Infrared (IR) spectroscopy spectra were collected on a Nicolet 330 FTIR Spectrometer within the 4000−400 cm^{-1} region. Thermogravimetric analysis (TGA) measurements were performed on a PerkinElmer TGA 7 instrument under a static N_2 atmosphere with a heating rate of 10 °C/min at the range of 40−900 °C. Gas-adsorption experiments were performed on the surface area analyzer ASAP-2020.

Scheme 1. Synthetic Procedures of the H_3ATTCA Ligand Materials and General Methods.

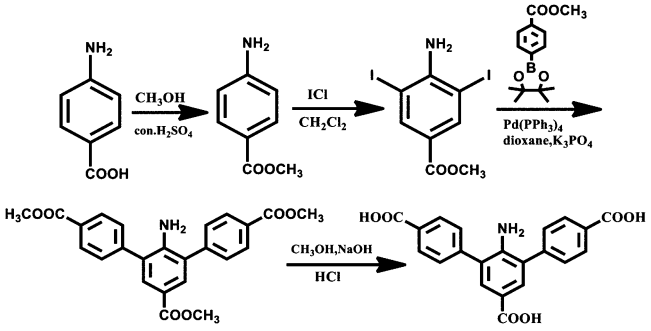

Scheme 2. Synthetic Procedures of the Complexes 1, 2, and UMCM-151

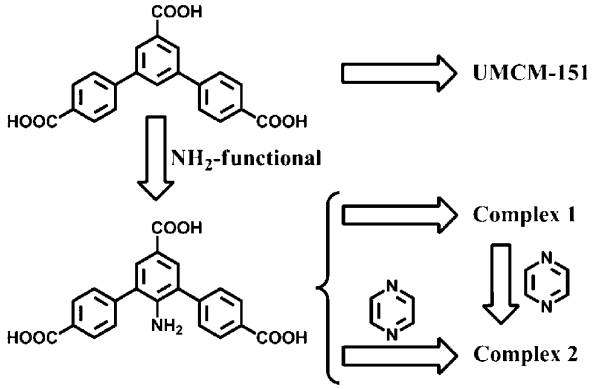

X-ray Structural Studies. X-ray diffraction data were collected on a Agilent Xcalibur Eos Gemini diffractometer with Mo Kα radiation (λ = 0.710 00 Å) at 293 K. All structures were solved by direct methods and refined by full-matrix least-squares on F^2 using *SHELXS-97*.[47] Non-hydrogen atoms were refined with anisotropic displacement parameters during the final cycles. Hydrogen atoms were placed in calculated positions with isotropic displacement parameters set to 1.2 × Ueq of the attached atom. The free solvent molecules in complexes **1** and **2** are highly disordered, and no satisfactory disorder model could be achieved. The *PLATON/SQUEEZE* routine was used to remove scattering from the disordered solvent molecules.[48,49] Table 1 shows pertinent crystallographic data collection and refinement parameters. Tables S1 and S2 shows selected bond angles and distances. Crystallographic data of **1** and **2** have been deposited with the Cambridge Crystallographic Data Center (CCDC: 1444849−1444850).

RESULTS AND DISCUSSION

Crystal Structures of Complexes 1−2. Single-crystal X-ray structural analysis demonstrates that **1** crystallizes in the orthorhombic space group of *Immm* and that its asymmetric unit consists of one deprotonated $ATTCA^{3-}$ ligand, one and a half copper ions, and one and a half coordinated water molecules. Cu1 atom is connected by four carboxylate oxygen atoms from four different $ATTCA^{3-}$ ligands and one oxygen atom from coordinated water molecule to generate a pentagonal pyramidal coordination geometry (Figure 1a). Adjacent Cu1 atoms are connected by four carboxyls to generate a $[Cu_2(COO)_4]$ paddlewheel subunit with the Cu1···Cu1 separation of 2.615 Å and Cu1−O bond length of 1.945 Å. Two different coordinated water molecules occupy the axial positions with the Cu1−O_{water} bond length of 2.179 Å (Table S1). In the similar paddlewheel $[Cu_2(COO)_4]$ subunits constructed by two Cu2 or two Cu3 atoms, the separations of Cu2···Cu2 and Cu3···Cu3 are 2.599 and 2.610 Å; the Cu2−O and Cu3−O average bond lengths are 1.905 and 1.942 Å; and the Cu2−O_{water} and Cu3−O_{water} bond distances are 2.123 and 2.205 Å, respectively. The three $Cu_2(COO)_4$ paddlewheel SBUs connected by $ATTCA^{3-}$ ligands to generate a noninterpenetrated three-dimensional (3D) network with large cavities as shown in Figure 1c. A hexagonal-shaped channel surrounded by six $ATTCA^{3-}$ ligands and four $Cu_2(COO)_4$ copper paddlewheel SBUs has the dimension of 31.1 Å × 7.4 Å viewed along the *a*-axis (Figure 1b), and two pentagonal-shaped channels surrounded by three $ATTCA^{3-}$ ligands and three $Cu_2(COO)_4$ paddlewheel SBUs have the dimensions of 17.3 Å × 7.0 and 16.8 Å × 7.0 Å, respectively, viewed along the *c*-axis (Figure 1d). PLATON[50] program analysis of **1** demonstrates that there is ∼73.7% solvent-accessible volume (23 183 $Å^3$). If the $Cu_2(COO)_4$ paddlewheel SBUs as a four-connected node, the $ATTCA^{3-}$ ligands as a three-connected planar linker, and the acetic acid groups as a two-connected node, obviously an ***fmj*** topology is employed by the 3D framework of **1** (Figure 1e).[51]

In **1**, the distance between the adjacent paddlewheel is 7.372 Å (Figure 1c), which is quite coincident with the length sum of pyrazine molecule (∼2.85 Å) and two Cu−N bonds (∼4.32 Å). Hence, the SCSC transformation from complex **1** to **2** was easily realized by adding pyz into the solution of **1**, and **2** keeps the same ***fmj*** topology. **2** crystallizes in the orthorhombic space group of *Immm*. One deprotonated $ATTCA^{3-}$ ligand, one and a half copper ions, half of a coordinated pyz molecule, and two coordinated water molecules can be observed in the asymmetric unit. The Cu2 atom is connected by four carboxylate oxygen atoms from four different $ATTCA^{3-}$ ligands and one nitrogen atom from coordinated pyz molecule to generate a pentagonal pyramidal coordination geometry (Figure 2a). Adjacent Cu2 atoms are connected by four

DOI: 10.1021/acs.inorgchem.6b00278
Inorg. Chem. 2016, 55, 6420−6425

Table 1. Crystal Data and Structure Refinements for Complexes 1, 2, and UMCM-151

identification code	**1**	**2**	**UMCM-151**
empirical formula	$C_{72}H_{138}Cu_3N_4O_{40}$	$C_{65}H_{114}Cu_3N_6O_{35}$	$C_{42}H_{26}Cu_3O_{15}$
formula weight	1890.33	1768.35	930.96
temperature/K	293(2)	293(2)	293(2)
crystal system	orthorhombic	orthorhombic	orthorhombic
space group	*Immm*	*Immm*	*Immm*
a/Å	34.1449(7)	34.1668(10)	33.8400(13)
b/Å	34.1449(7)	34.1668(10)	33.8400(13)
c/Å	19.8843(12)	19.3425(9)	21.699(4)
α/deg	90.00	90.00	90.00
β/deg	90.00	90.00	90.00
γ/deg	90.00	90.00	90.00
volume/Å^3	23182.6(16)	22579.9(14)	24848(5)
Z	8	8	8
ρ_{calc}, mg/mm^3	0.569	0.609	0.498
m, mm^{-1}	0.570	0.586	0.536
F(000)	4024.0	4184.0	3656.0
radiation	Mo K*α* (*λ* = 0.710 00)	Mo K*α* (*λ* = 0.710 00)	Mo K*α* (*λ* = 0.710 00)
2Θ range for data collection	6.08 to 52.68°	3.36 to 51.56°	3.28 to 51.44°
reflections collected	74 379	22 252	23 926
independent reflections	12 610 [Rint = 0.1575, Rsigma = 0.1587]	9724 [Rint = 0.1347, Rsigma = 0.3225]	11 162 [Rint = 0.0663, Rsigma = 0.1081]
data/restraints/parameters	12 610/2/314	9724/7/308	11 162/0/292
goodness-of-fit on F^2	0.902	0.652	0.803
final *R* indexes [$I > 2\sigma(I)$]	R_1 = 0.1105, wR_2 = 0.2785	R_1 = 0.0928, wR_2 = 0.2145	R_1 = 0.1085, wR_2 = 0.2816
final *R* indexes [all data]	R_1 = 0.2214, wR_2 = 0.3183	R_1 = 0.2042, wR_2 = 0.2597	R_1 = 0.1650, wR_2 = 0.3062

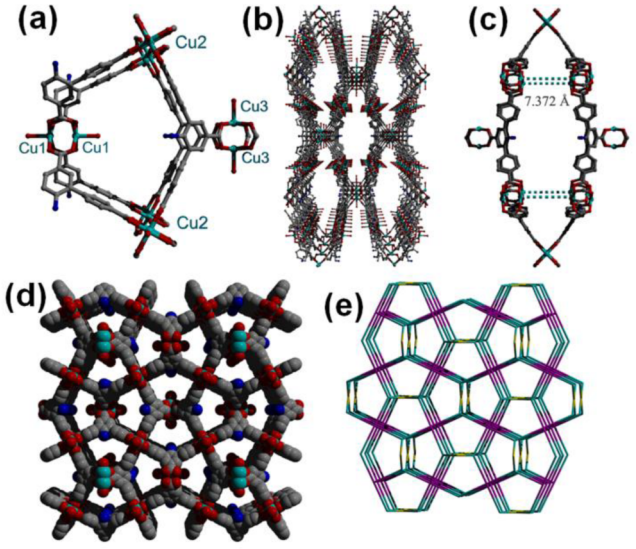

Figure 1. (a) Coordination situation of $Cu_2(COO)_4$ paddlewheel in **1** and the linkmode of H_3ATTCA. (b) Projection view of 3D open framework along the *a* axis, showing the rhombic channels. (c) The single cavity of **1**. (d) 3D porous non-interpenetrating framework viewed along the *c* axis. (e) The ***fmj*** topological net.

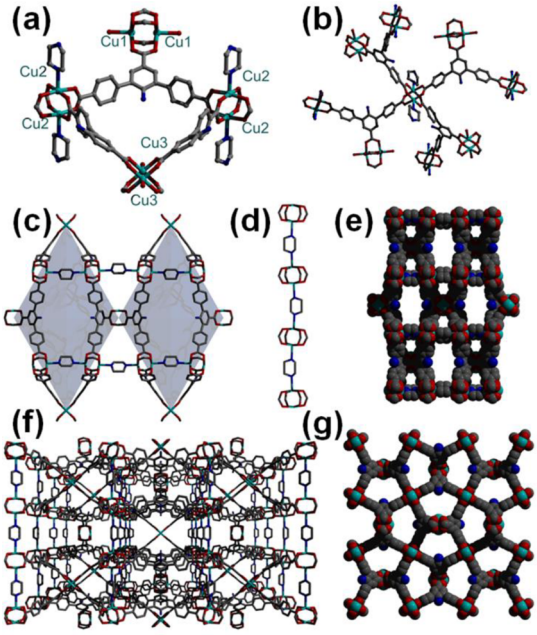

Figure 2. (a, b) Coordination situation of $Cu_2(COO)_4$ paddlewheel in **2** and the linkmode of H_3ATTCA and pyz. (c) The rhombic cavity of **2**. (d) $Cu_2(COO)_4$ paddlewheel linked by pyz formed 1D chain structure. (e–g) 3D porous non-interpenetrating network viewed from the *a*, *b*, and *c* axes.

carboxyls to generate a $[Cu_2(COO)_4]$ paddlewheel subunit with a Cu2···Cu2 separation of 2.584 Å, and the average Cu2–O bond length is 1.983 Å; the Cu2–N bond length is 2.159 Å. The two axial sites of each paddlewheel SBU are occupied by pyz molecules instead of coordinated water molecules in **1** (Figure 2a,b). In the paddlewheel SBUs formed by two Cu1 or Cu3 atoms, the separations of Cu1–Cu1 and Cu3–Cu3 are 2.590 and 2.630 Å, respectively, and the average Cu1–O bond length is 1.993 Å, the average Cu3–O bond length is 1.938 Å. Two coordinated water molecules occupy the axial positions with the Cu1–O_{water} and Cu3–O_{water} bond length of 2.254 and 2.23 Å, respectively. Along the *c* axis, pyz ligand connects two adjacent Cu2 paddlewheel subunits to generate an infinite one-dimensional (1D) chain (Figure 2d).

The $Cu_2(COO)_4$ paddlewheel SBUs are connected by $ATTCA^{3-}$ ligands to generate a non-interpenetrated 3D network with large cavities (Figure 2c). A hexagonal-shaped

DOI: 10.1021/acs.inorgchem.6b00278
Inorg. Chem. 2016, 55, 6420–6425

channel can be observed along the *a* axis, but it was separated into two parts by coordinated pyz molecules: the bigger pore is surrounded by two $ATTCA^{3-}$ ligands, two pyz molecules, and four $Cu_2(COO)_4$ paddlewheel SBUs with a dimension of 16.8 Å × 7.1 Å, and the smaller pore can be observed along the *b* axis with a dimension of 7.6 Å × 7.1 Å, which is formed through the connection of two $ATTCA^{3-}$ groups, one pyz molecule, and three $Cu_2(COO)_4$ paddlewheel SBUs (Figure 2e). Moreover, along the *c* axis, two large pentagonal-shaped channels surrounded by three $ATTCA^{3-}$ ligands and three $Cu_2(COO)_4$ paddlewheel SBUs can be observed with the dimensions of 17.3 Å × 8.26 and 16.8 Å × 9.25 Å, which are slightly larger than those in **1** (Figure 2g). The *PLATON*[50] program analysis of **2** demonstrates that there is ~71.7% of the solvent-accessible volume (22 580 $Å^3$), which is smaller than the value of **1**, as coordinated pyz molecules are partially stacked in the pores.

UMCM-151 $[Cu_2(C_{21}H_{11}O_6)_{1.33}]$ has been reported by Matzger's group using nonamino-functional ligand of H_3TTCA.[45] Similar to **1** and **2**, it keeps the same ***fmj*** topology and possesses open porous network, which crystallizes in the orthorhombic space group of *Immm*. Three crystallographically independent copper atoms can be observed in the asymmetric unit. The coordination situation of **UMCM-151** is same as **1**. Along the *a*, *b*, and *c* axes, three pentagonal-shaped channels were observed with the dimensions of 11.4 × 9.6 Å, 11.3 × 6.9 Å, and 28.4 × 11.0 Å, respectively (Figure S4). The *PLATON*[50] program analysis of **UMCM-151** demonstrates that there is ~76.6% solvent-accessible volume (24 848 $Å^3$), which is greater than **1** and **2**, as no amino groups stacked in the holes.

Gas-Adsorption of Complexes 1, 2, and UMCM-151. Considering the existence of 3D channels, gas-uptake measurements for desolvated **1**, **2**, and **UMCM-151** were performed. Before the measurement, the as-synthesized crystal samples of **1**, **2**, and **UMCM-151** were immersed in methanol to exchange the uncoordinated DMF, EtOH, and water moleculers. Then drying was done at 60 °C under high vacuum for 3 h to get the activated samples.

As shown in Figure 3, complex **1** exhibits a typical type-I isotherm for N_2 at 77 K, with the Brunauer–Emmett–Teller (BET) surface area of 746.19 $m^2 \cdot g^{-1}$ and the adsorption abilities of 213.62 $cm^3 \cdot g^{-1}$, indicating its permanent porosity.[52,53] The adsorption capacities for H_2 are 131.38 and 91.08 $cm^3 \cdot g^{-1}$ at 77 and 87 K, respectively (Figure 3b and Table 2),

Table 2. Gas-Adsorption Data for Complexes 1, 2, and UMCM-151

gas	complex	*T*	*V* abs [$cm^3 \cdot g^{-1}$]	amount [$mmol \cdot g^{-1}$]	[wt %]
N_2	**1**	77 K	213.62	9.54	26.71
	2	77 K	138.24	6.17	17.27
	UMCM-151	77 K	195.67	8.74	24.47
H_2	**1**	77 K	131.38	5.86	1.17
	1	87 K	91.08	4.07	0.81
	2	77 K	83.75	3.74	0.75
	2	87 K	60.73	2.71	0.54
	UMCM-151	77 K	106.67	4.76	0.95
	UMCM-151	87 K	63.59	2.84	0.57
CO_2	**1**	273 K	85.92	3.83	16.85
	1	298 K	49.63	2.21	9.72
	2	273 K	53.30	2.38	10.47
	2	298 K	30.80	1.37	6.03
	UMCM-151	273 K	55.97	2.50	11.00
	UMCM-151	298 K	22.28	0.99	4.36
C_2H_2	**1**	273 K	87.50	3.91	10.17
	2	273 K	68.50	3.06	7.96
	UMCM-151	273 K	49.91	2.23	5.80
CH_4	**1**	273 K	22.79	1.02	1.63
	2	273 K	17.18	0.77	1.23
	UMCM-151	273 K	10.47	0.47	0.75

which is larger than **UTSA-36** with a similar BET surface area[54] of 806 $m^2 \cdot g^{-1}$ and a H_2 adsorption capacity of 123.00 $cm^3 \cdot g^{-1}$ (1.1 wt %) at 77 K.[55] The adsorption capacities for CO_2, C_2H_2, and CH_4 are 85.92, 87.50, and 22.79 $cm^3 \cdot g^{-1}$ at 273 K, whereas CO_2 at 298 K is 49.63 $cm^3 \cdot g^{-1}$.

As shown in Figure 4, the maximum adsorption capacity of **2** is 138.24 $cm^3 \cdot g^{-1}$ for N_2 at 77 K. The adsorption capacities for H_2 are 83.75 and 60.73 $cm^3 \cdot g^{-1}$ at 77 and 87 K, respectively (Figure 4b and Table 2). The adsorption capacities for CO_2,

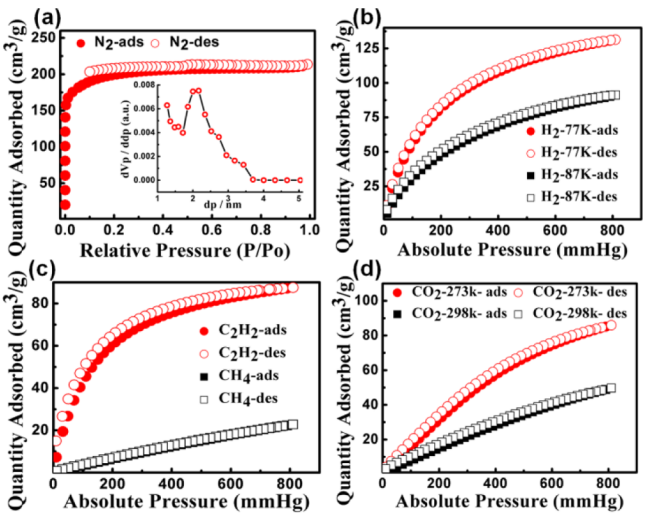

Figure 3. Gas-adsorption isotherms for **1**: (a) N_2 at 77 K; (b) H_2 at 77 and 87 K; (c) C_2H_2 and CH_4 at 273 K; (d) CO_2 at 273 and 298 K.

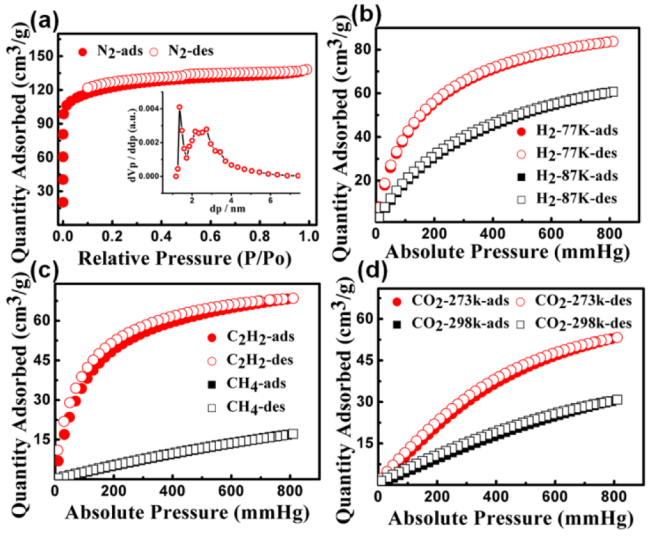

Figure 4. Gas-adsorption isotherms for **2**: (a) N_2 at 77 K; (b) H_2 at 77 and 87 K; (c) C_2H_2 and CH_4 at 273 K; (d) CO_2 at 273 and 298 K.

DOI: 10.1021/acs.inorgchem.6b00278
Inorg. Chem. 2016, 55, 6420–6425

C_2H_2, and CH_4 are 53.30, 68.50, and 17.18 $cm^3 \cdot g^{-1}$ at 273 K, whereas CO_2 at 298 K is 30.80 $cm^3 \cdot g^{-1}$. The adsorption abilities for **2** are quite obviously lower than those of **1**, which is attributed to the introduced pyz having partially occupied the pores of **2**.

As shown in Figure 5, the maximum adsorption capacity of **UMCM-151** is 195.67 $cm^3 \cdot g^{-1}$ for N_2 at 77 K. The adsorption

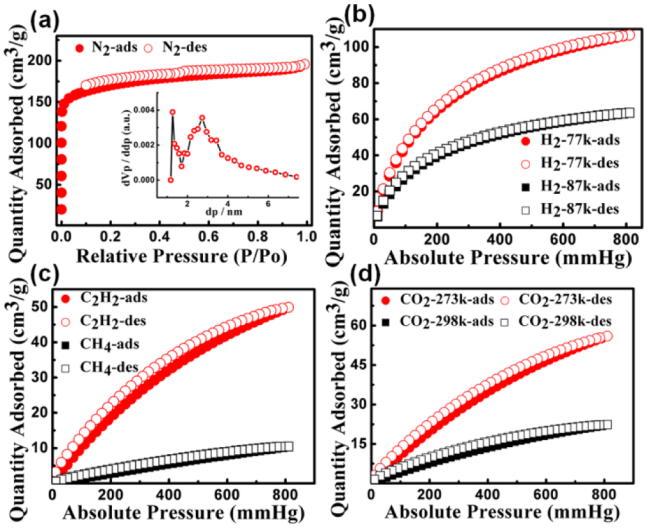

Figure 5. Gas-adsorption isotherms for **UMCM-151**: (a) N_2 at 77 K; (b) H_2 at 77 and 87 K; (c) C_2H_2 and CH_4 at 273 K; (d) CO_2 at 273 and 298 K.

capacities for H_2 are 106.67 and 63.59 $cm^3 \cdot g^{-1}$ at 77 and 87 K, respectively (Figure 5b and Table 2). The adsorption capacities for CO_2, C_2H_2, and CH_4 are 55.97, 49.91, and 10.47 $cm^3 \cdot g^{-1}$ at 273 K, whereas CO_2 at 298 K is 22.28 $cm^3 \cdot g^{-1}$. Although the pores of **UMCM-151** are larger than those of **1**, the lower gas adsorption of **UMCM-151** is easily attributed to the introduced polar groups (NH_2-) located at MOF channels, which can significantly improve the CO_2 adsorption capacity and gas-adsorption selectivity. Amino groups play a role of Lewis base to form the active sites on the tunnel walls, which have strong interactions with Lewis acid (CO_2 and C_2H_2). On the basis of the above results, we can conclude that the introduction of amino not only can occupy part of the channel structure but also can improve the gas-adsorption ability, just like a "double-edged sword".

The virial-type expression was used to calculate H_2 and CO_2 gas isosteric heat of adsorption (Q_{st}).[56] By fitting the H_2 adsorption isotherms at 77 and 87 K, the Q_{st} for H_2 was obtained with the estimated value of 6.2 kJ mol^{-1} for **1** and 6.6 kJ mol^{-1} for **2**, which are higher than that of **UMCM-151** (4.9 kJ mol^{-1}; Figures S12–S14). By fitting the CO_2 adsorption isotherms at 273 and 298 K, the Q_{st} for CO_2 was obtained with the estimated value of 19.0 kJ mol^{-1} for **1** and 24.1 kJ mol^{-1} for **2** (Figures S12 and S13). The value is lower than that of **UMCM-151** (29.0 kJ mol^{-1}; Figure S14), similar to those of **UMCM-150** (20.6 kJ mol^{-1}), **MIL-47** (20.8 kJ mol^{-1}), and **HKUST-1** (25.1 kJ mol^{-1}), but higher than those values for **MOF-177** (15.7 kJ mol^{-1}), **IRMOF-1** (15.8 kJ mol^{-1}), and **UMCM-1** (15.5 kJ mol^{-1}).[57,58]

CONCLUSIONS

Two amino-functional MOFs based on $Cu_2(COO)_4$ paddle-wheel SBUs were successfully synthesized. By replacing the coordinated water molecule with pyz molecule, the SCSC transformation of complex **1** to **2** was realized. Both complexes **1** and **2** show an ***fmj*** topology. The adsorption abilities of **2** are lower than that of **1**, as part of the pores is stacked by pyz in **2**. Compared with **UMCM-151**, the amino-functional **1** shows the higher gas-adsorption capacity for N_2, H_2, CO_2, CH_4, and C_2H_2, especially for CO_2. This behavior further confirmed that the amino-functional MOFs can significantly improve the CO_2 adsorption capacity and selectivity, as the polar amino groups in the tunnel walls can form the strong Lewis acid–base interactions with the Lewis acid (CO_2 and C_2H_2). Further research work based on the amino-functional modification ligand and potential application in gas storage or CO_2 removal from the natural gas are underway in our lab.

ASSOCIATED CONTENT

Supporting Information

The Supporting Information is available free of charge on the ACS Publications website at DOI: 10.1021/acs.inorgchem.6b00278.

Detailed synthetic procedures, selected bond angles and lengths, ^1H NMR spectrum, crystal structures of **UMCM-151**, TGA curves, IR curves, PXRD patterns, isosteric adsorption enthalpy (PDF)

X-ray crystallographic information (CIF)

X-ray crystallographic information (CIF)

AUTHOR INFORMATION

Corresponding Authors

*E-mail: fndai@upc.edu.cn. (F.D.)

*E-mail: liangliangzhang@upc.edu.cn. (L.Z.)

*E-mail: luolw@upc.edu.cn. (L.L.)

Funding

This work was supported by the China Postdoctoral Science Foundation (2012M510172), the NSFC (Grant Nos. 21371179 and 21201179), the Foundation of State Key Laboratory of Structural Chemistry (20160006), and the Fundamental Research Funds for the Central Universities (14CX02213A and 16CX05015A).

Notes

The authors declare no competing financial interest.

REFERENCES

(1) Zhou, H. C.; Long, J. R.; Yaghi, O. M. *Chem. Rev.* **2012**, *112*, 673–674.

(2) Zhang, J. P.; Zhang, Y. B.; Lin, J. B.; Chen, X. M. *Chem. Rev.* **2012**, *112*, 1001–1033.

(3) Liu, T. F.; Feng, D. W.; Chen, Y. P.; Zou, L. F.; Bosch, M.; Yuan, S.; Wei, Z. W.; Fordham, S.; Wang, K. C.; Zhou, H. C. *J. Am. Chem. Soc.* **2015**, *137*, 413–419.

(4) Lin, Q. P.; Bu, X. H.; Kong, A. G.; Mao, C. Y.; Zhao, X.; Bu, F.; Feng, P. Y. *J. Am. Chem. Soc.* **2015**, *137*, 2235–2238.

(5) Wang, X. Q.; Zhang, L. L.; Yang, J.; Liu, F. L.; Dai, F. N.; Wang, R. M.; Sun, D. F. *J. Mater. Chem. A* **2015**, *3*, 12777–12785.

(6) Beauvais, L. G.; Shores, M. P.; Long, J. R. *J. Am. Chem. Soc.* **2000**, *122*, 2763–2772.

(7) Chen, L.; Yang, Y.; Guo, Z.; Jiang, D. *Adv. Mater.* **2011**, *23*, 3149–3154.

(8) Chandler, B. D.; Yu, J. O.; Cramb, D. T.; Shimizu, G. K. H. *Chem. Mater.* **2007**, *19*, 4467–4473.

DOI: 10.1021/acs.inorgchem.6b00278
Inorg. Chem. 2016, 55, 6420–6425

(9) Allendorf, M. D.; Bauer, C. A.; Bhakta, R. K.; Houk, R. J. T. *Chem. Soc. Rev.* **2009**, *38*, 1330−1352.
(10) Maspoch, D.; Domingo, N.; Roques, N.; Wurst, K.; Tejada, J.; Rovira, C.; Ruiz-Molina, D.; Veciana, J. *Chem. - Eur. J.* **2007**, *13*, 8153−8163.
(11) Roques, N.; Mugnaini, V.; Veciana, J. *Magnetic and Porous Molecule-Based Materials. In Functional Metal-Organic Frameworks: Gas Storage, Separation and Catalysis;* Springer: New York, 2010; Vol. *293*, p 207.
(12) Kurmoo, M. *Chem. Soc. Rev.* **2009**, *38*, 1353−1379.
(13) Zeng, Y. F.; Hu, X.; Liu, F. C.; Bu, X. H. *Chem. Soc. Rev.* **2009**, *38*, 469−480.
(14) Moore, D. S. *Rev. Sci. Instrum.* **2004**, *75*, 2499−2512.
(15) Takats, Z.; Cotte-Rodriguez, I.; Talaty, N.; Chen, H.; Cooks, R. G. *Chem. Commun.* **2005**, 1950−1952.
(16) Zhao, X.; Xiao, B.; Fletcher, A. J.; Thomas, K. M.; Bradshaw, D.; Rosseinsky, M. J. *Science* **2004**, *306*, 1012−1015.
(17) Das, S.; Kim, H.; Kim, K. *J. Am. Chem. Soc.* **2009**, *131*, 3814−3815.
(18) Perry, J. J.; Perman, J. A.; Zaworotko, M. J. *Chem. Soc. Rev.* **2009**, *40*, 3018−3032.
(19) Abrahams, B. F.; Hardie, M. J.; Hoskins, B. F.; Robson, R.; Williams, G. A. *J. Am. Chem. Soc.* **1992**, *114*, 10641−10643.
(20) Abrahams, B. F.; Hoskins, B. F.; Michail, D. M.; Robson, R. *Nature* **1994**, *369*, 727−728.
(21) Liu, D.; Lang, J.-P.; Abrahams, B. F. *J. Am. Chem. Soc.* **2011**, *133*, 11042−11045.
(22) Yuan, S.; Deng, Y. K.; Sun, D. *Chem. - Eur. J.* **2014**, *20*, 10093−10098.
(23) Yang, J.; Wang, X. Q.; Dai, F. N.; Zhang, L. L.; Wang, R. M.; Sun, D. F. *Inorg. Chem.* **2014**, *53*, 10649−10653.
(24) Chen, C.; Allen, C. A.; Cohen, S. M. *Inorg. Chem.* **2011**, *50*, 10534−10536.
(25) Zhang, J. P.; Chen, X. M. *J. Am. Chem. Soc.* **2009**, *131*, 5516−5521.
(26) Zheng, B. S.; Bai, J. F.; Duan, J. G.; Wojtas, L.; Zaworotko, M. J. *J. Am. Chem. Soc.* **2011**, *133*, 748−751.
(27) McDonald, T. M.; Lee, W. R.; Mason, J. A.; Wiers, B. M.; Hong, C. S.; Long, J. R. *J. Am. Chem. Soc.* **2012**, *134*, 7056−7065.
(28) Planas, N.; Dzubak, A. L.; Poloni, R.; Lin, L.-C.; McManus, A.; McDonald, T. M.; Neaton, J. B.; Long, J. R.; Smit, B.; Gagliardi, L. *J. Am. Chem. Soc.* **2013**, *135*, 7402−7405.
(29) McDonald, T. M.; D'Alessandro, D. M.; Krishna, R.; Long, J. R. *Chem. Sci.* **2011**, *2*, 2022−2028.
(30) Chui, S. S.-Y.; Lo, M.-F.; Charmant, J. P. H.; Orpen, A. G.; Williams, I. D. *Science* **1999**, *283*, 1148−1150.
(31) He, Y.; Zhang, Z.; Xiang, S.; Fronczek, F. R.; Krishna, R.; Chen, B. *Chem. - Eur. J.* **2012**, *18*, 613−619.
(32) Ma, S.; Sun, D.; Ambrogio, M.; Fillinger, J. A.; Parkin, S.; Zhou, H. C. *J. Am. Chem. Soc.* **2007**, *129*, 1858−1859.
(33) Furukawa, H.; Go, Y. B.; Ko, N.; Park, Y. K.; Uribe-Romo, F. J.; Kim, J.; O'Keeffe, M.; Yaghi, O. M. *Inorg. Chem.* **2011**, *50*, 9147−9152.
(34) Guo, D.; McCusker, J. K. *Inorg. Chem.* **2007**, *46*, 3257−3274.
(35) Baum, A.; Lindeman, S. V.; Fiedler, A. T. *Chem. Commun.* **2013**, *49*, 6531−6533.
(36) Hou, C.; Liu, Q.; Fan, J.; Zhao, Y.; Wang, P.; Sun, W. Y. *Inorg. Chem.* **2012**, *51*, 8402−8408.
(37) Zhang, P.; Li, B.; Zhao, Y.; Meng, X.; Zhang, T. *Chem. Commun.* **2011**, *47*, 7722−7724.
(38) Liu, X.; Oh, M.; Lah, M. S. *Inorg. Chem.* **2011**, *50*, 5044−5053.
(39) Eubank, J. F.; Wojtas, L.; Hight, M. R.; Bousquet, T.; Kravtsov, V.; Eddaoudi, M. *J. Am. Chem. Soc.* **2011**, *133*, 17532−17535.
(40) Chakrabarty, R.; Mukherjee, P. S.; Stang, P. J. *Chem. Rev.* **2011**, *111*, 6810−6918.
(41) Inukai, M.; Fukushima, T.; Hijikata, Y.; Ogiwara, K.; Horike, S.; Kitagawa, S. *J. Am. Chem. Soc.* **2015**, *137*, 12183−12186.
(42) Brega, V.; Zeller, M.; He, Y. F.; Lu, H. P.; Klosterman, J. K. *Chem. Commun.* **2015**, *51*, 5077−5080.
(43) Corey, E. J. *Chem. Soc. Rev.* **1988**, *17*, 111−133.
(44) Wu, G. P.; Wei, S. H.; Ren, W. M.; Lu, X. B.; Xu, T. Q.; Darensbourg, D. J. *J. Am. Chem. Soc.* **2011**, *133*, 15191−15199.
(45) Schnobrich, J. K.; Lebel, O.; Cychosz, K. A.; Dailly, A.; Wong-Foy, A. G.; Matzger, A. J. *J. Am. Chem. Soc.* **2010**, *132*, 13941−13948.
(46) Li, F. R.; Yang, S. I.; Ciringh, Y.; Seth, J.; Martin, C. H.; Singh, D. L.; Kim, D.; Birge, R. R.; Bocian, D. F.; Holten, D.; Lindsey, J. S. *J. Am. Chem. Soc.* **1998**, *120*, 10001−10017.
(47) Sheldrick, G. M. A *Program for X-ray Crystal Structure Refinement;* University of Gottingen: Germany, 1997.
(48) Spek, A. L. PLATON, *A multipurpose crystallographic tool;* Utrecht University: The Netherlands, 2001.
(49) Sheldrick, G. M. *Acta Crystallogr., Sect. A: Found. Crystallogr.* **2008**, *64*, 112−122.
(50) Spek, A. *J. Appl. Crystallogr.* **2003**, *36*, 7−13.
(51) O'Keeffe, M.; Yaghi, O. M. *Reticular Chemistry Structure Resource*, Arizona State University: Tucson, 2005. Please see the Web site of the O'Keeffe group at Arizona State University, http://rcsr.anu.edu.au.
(52) Smith, M. K.; Northrop, B. H. *Chem. Mater.* **2014**, *26*, 3781−3795.
(53) Zhao, Y.; Yao, K. X.; Teng, B.; Zhang, T.; Han, Y. *Energy Environ. Sci.* **2013**, *6*, 3684−3692.
(54) Yang, J.; Wang, X. Q.; Dai, F. N.; Zhang, L. L.; Wang, R. M.; Sun, D. F. *Inorg. Chem.* **2014**, *53*, 10649−10653.
(55) Suh, M. P.; Park, H. J.; Prasad, T. K.; Lim, D. W. *Chem. Rev.* **2012**, *112*, 782−835.
(56) Czepirski, L.; Jagiello, J. *Chem. Eng. Sci.* **1989**, *44*, 797−801.
(57) Babarao, R.; Jiang, J. *Langmuir* **2008**, *24*, 6270−6278.
(58) Yazaydin, A. O.; Snurr, R. Q.; Park, T.-H.; Koh, K.; Liu, J.; Levan, M. D.; Benin, A. I.; Jakubczak, P.; Lanuza, M.; Galloway, D. B.; Low, J. J.; Willis, R. R. *J. Am. Chem. Soc.* **2009**, *131*, 18198−18199.

DOI: 10.1021/acs.inorgchem.6b00278
Inorg. Chem. 2016, 55, 6420−6425